Contribution of DFT Calculations to the Understanding of an Asymmetric Reaction, the Hydrogen Transfer Reduction of Ketones by a Rhodium(I) Complex

Françoise Delbecq,*[a,b] Vincent Guiral,[a] and Philippe Sautet[a]

Keywords: Acetophenone / Density functional calculations / Enantioselectivity / Hydrogen transfer / Rhodium(I) complex

The density functional theory (DFT) calculations presented here allow us to understand the mechanism of an asymmetric reaction, the hydride transfer reduction of acetophenone by a Rh^I complex bearing a chiral diamine ligand, RhH(diam)-(COD). The mechanism which accounts for the enantioselectivity is a concerted one, where both the hydride and one hydrogen carried by a nitrogen are transferred simultaneously to the ketone. The two diastereoisomeric transition states leading to the *R* and *S* alcohols have been determined, the former being the most stable. The activation free energies, the kinetic constants and the enantiomeric excesses *ee* have been calculated, giving values in good agreement with the experiments.

Two conditions ensure the enantioselectivity. The first is the existence of a unique isomer of the starting complex, which is achieved by the presence of bulky substituents on the diamine asymmetric carbons. The second is the presence of one hydrogen on the diamine nitrogens (secondary amines) and the existence of a C_2 axis for the diamine ligand, which means that only one of these hydrogens points in the same direction as the Rh–H bond, a condition necessary for a low-energy concerted transfer.

I. Introduction

The synthesis of optically pure chiral compounds is a key process for the chemical and pharmaceutical industries. The catalytic asymmetric hydrogen transfer reaction allows the reduction of prochiral ketones into optically active alcohols. Complexes of transition metals like Ru^{II}, Rh^I, or Ir^I bearing chiral ligands are often used.[1,2] Phosphorus ligands are the most common; however, nitrogen-containing ligands show remarkable catalytic performances and have been widely studied in the last decade.[3−9] Nevertheless little was known about the reaction steps, except for the X-ray determination of intermediates with Ru^{II} catalysts[10,11] and a kinetic study in the case of a Rh^I catalyst.[12] Only a few papers deal with the theoretical study of the mechanism of the asymmetric reduction of ketones. One can cite two reactions catalyzed by Ru^{II} complexes.[13,14] In the latter work, the enantiomeric transition states are calculated.

We have focused our attention on the asymmetric reduction of acetophenone by a complex of Rh^I bearing a chiral diamine as ligand (see Scheme 1).[4,5,7,9] When the chiral diamine is the (*S*,*S*)-*N*,*N*′-dimethyl-1,2-diphenylethylenediamine, the (*R*)-phenylethanol is obtained with an enantiomeric excess *ee* in the range 40−67% depending on the experimental conditions: for instance, in the conditions

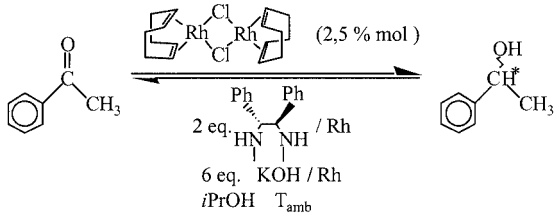

Scheme 1

shown on Scheme 1, *ee* is 40%. When the cyclooctadiene is replaced by two ethylene molecules, *ee* increases to 50%.[9]

In our previous papers, we have presented density functional theory (DFT) calculations on the mechanism of this reaction. We have compared a step-wise mechanism[15] and a concerted one.[16] We have shown that the latter was the most probable and the one able to explain the enantioselectivity of the reaction. This concerted mechanism is similar to the one found for the same reaction catalyzed by a Ru^{II} complex.[9,13] In these studies with Rh^I we have considered a model complex having no substituent on the carbons of the diamine. In the present work we complete our study by considering a Rh^I complex with the real diamine as ligand, bearing phenyl groups on the carbon atoms. At the same

[a] Institut de Recherches sur la Catalyse,
2 avenue A. Einstein, 69626 Villeurbanne Cedex, France
[b] Laboratoire de Chimie Théorique, Ecole Normale Supérieure,
46 allée d′Italie, 69364 Lyon Cedex 07, France
Fax: (internat.) +33-4-72445399
E-mail: delbecq@catalyse.cnrs.fr

  DOI: 10.1002/ejoc.200200701

time our purpose is also to present a summary of the factors that control the enantioselectivity of the reaction. Furthermore, calculations of the vibrational frequencies have allowed us to obtain the activation free energies and hence the kinetic constants. The ratio of these constants for the isomeric pathways is directly related to *ee*.

Therefore we will firstly briefly recall our previous results, then present the study with the experimental complex and finally set out the kinetic part of our work.

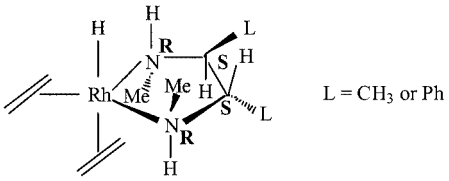

Scheme 2

II. Computational Methods

The calculations were based on density functional theory (DFT) at the generalized gradient approximation (GGA) level. They were performed with the Gaussian98 code.[17] We used the GGA PW91 and the hybrid B3LYP functionals. For the Rh atom, we used the relativistic effective core potential of Hay and Wadt (with 4s and 4p in the valence) and the corresponding double ζ basis set.[18] A pseudopotential was also used for C, N, and O atoms.[19] The corresponding double ζ valence basis set was of 41G type[20] with a d polarization function on N (α = 0.80), C (α = 0.75), and O (α = 0.85). For H atoms, we used the Duning double ζ basis set with a 2p polarization orbital on the hydride (α = 1.0).

Geometries of reactants and products were fully optimized without any constraints. Transition-state geometries were found via the quasi-Newton algorithms,[21] QST2 or QST3. A vibrational characterization of all the transition states was performed.

III. Enantioselective Mechanism

1. Structure of the Initial Complex

We have shown previously[9] that the reactive complex has only one diamine ligand and keeps a diene ligand (COD) which has been modeled by two ethylene molecules. The experimental diamine, which gives the asymmetric reaction, has one methyl group on each nitrogen atom and one phenyl group on each carbon atom in a *meso* configuration. Initially we studied the influence of the nature of the substituents on the carbons[22] and compared L = methyl and L = phenyl (see Scheme 2). The complex with L = Ph and two ethylene ligands is one of the experimental complexes.[9] With one substituent on each atom of the diamine, there are 16 diastereoisomeric complexes. Optimization of all these isomers showed that two of them are more stable than the others. For L = CH_3, they only differ by 0.6 kcal/mol (see Table 1) which means that they coexist in the reaction medium. For L = Ph, the energy difference is larger (2.6 kcal/mol) which is sufficient for us to assert that diastereoisomer **1** is largely predominant. In this complex, the substituents are arranged alternately above and below the mean plane of the diamine, giving a C_2 symmetry axis.

Table 1. Relative energies of the two most stable diastereoisomers of the hydride complex depending on substituent L (in kcal/mol), obtained with the BPW91 functional

	L = Me	L = Ph
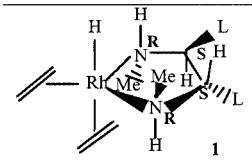 **1**	0	0
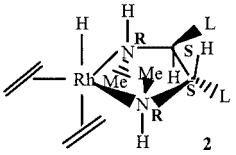 **2**	0.6	2.6

The total energy can be decomposed into two terms: the deformation energy necessary to bring the free diamine into a geometry allowing the coordination and the interaction energy between the deformed diamine and the metallic fragment. We have shown that the relative stability of the various diastereoisomers does not result only from steric effects.[22] Indeed, compared to structure **1**, the configuration of the diamine where the phenyls are *axial* and *cis* relative to the methyl groups has a similar deformation energy, which is surprising. However structure **1** is favored by a much larger interaction energy with the rhodium. Hence the stability of the complexes is not only governed by an adequate arrangement of the substituents of the diamine but by the strength of the interactions between the fragment orbitals.

In conclusion, the presence of phenyls on the carbons of the diamine assures the existence of only one privileged isomer for the reactive complex. If methyl groups are used instead, two isomers can coexist and both can react with the ketone, yielding a less-controlled reaction.

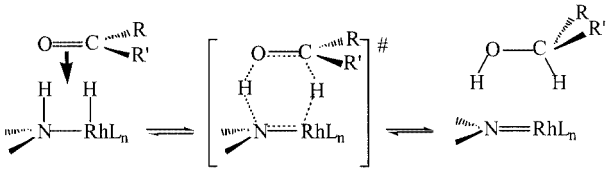

Scheme 3

2. Reactivity and Search of Transition States

As presented in the introduction, we have shown[15,16] that the mechanism of this asymmetric hydrogenation is a concerted one involving the hydride and a hydrogen of the diamine (Scheme 3).

When acetophenone approaches the complex, a hydrogen bond is formed between the oxygen and the hydrogen of one amine function. The product resulting from the transfer of two hydrogens on acetophenone is 2-propanol, bound to the rhodium complex by a hydrogen bond between N and O−H. These two complexes, reactant and product, have been optimized in the case of L = H[15] and L = Ph (this work). In the case of L = H, the carbon atoms of the diamine are no longer asymmetric but we have kept for the nitrogens the same unique configuration as determined for the initial complex. This means that the nitrogen atoms have an *R* configuration with an axial hydrogen on each. One of these hydrogens points toward the Rh−H bond. This is a model for the molecule with L = Ph, freezing the constraint of substituents on the ligand structure, but eliminating the specific interactions of these phenyl substituents with the incoming substrate. This is only a model and not a realistic system since in the case of a nonchiral ligand, the other configuration of the nitrogen atoms is of course equally probable, resulting in a strictly nil *ee*.

Acetophenone is a pro-chiral ketone and two possibilities exist for the approach, depending on the position of the two substituents (either CH_3 or Ph is behind). The precursor and the product for the two possible approaches are depicted in Figure 1 in the case of L = Ph. The bond lengths between the interacting atoms are given. In the *S* precursor, the hydrogen bond between O and H is shorter but the distance between C and the hydride is larger owing to steric hindrance between the methyl of acetophenone and the methyl carried by the second nitrogen. The energies are given in Table 2. Both the coordinated reactant and product are more stable for path *R* than for path *S*, with a small energy difference.

With a knowledge of the precursors and of the products, the *R* and the *S* transition states (TS) have been located in both cases, L = H and L = Ph. The geometry of these TS is also given in Figure 1 for L = Ph. The bond lengths are similar to those found previously without phenyls.[16] The transition state leading to the *S* isomer is earlier on the reaction path: the C−O and N−H bonds are less elongated and the C−H and O−H bonds are longer. The key difference is for the C−H bond being formed (0.11 Å between *R* and *S* transition states). This is explained by the through-space interaction between the methyl group on acetophenone and the one carried by the N atom not directly involved in the reaction. The alternating substituents in the diamine ligand structure for the most stable isomer of the initial complex ensures that this methyl is pointing upward, and hence can partially hinder the approach of the ketone leading to the *S* product. The shortest H−H distance between the two methyls is 2.6 Å for L = H and 2.4 Å for L = Ph. In the transition state leading to the *R* product, this methyl group is facing the phenyl ring of the incoming reactant and the steric repulsion is weaker since the shortest C−H distance is 3.2 Å for L = H and 2.9 Å for L = Ph. In the case of L = Ph, the oxygen of the acetophenone is not very far from a hydrogen of one of the phenyls of the

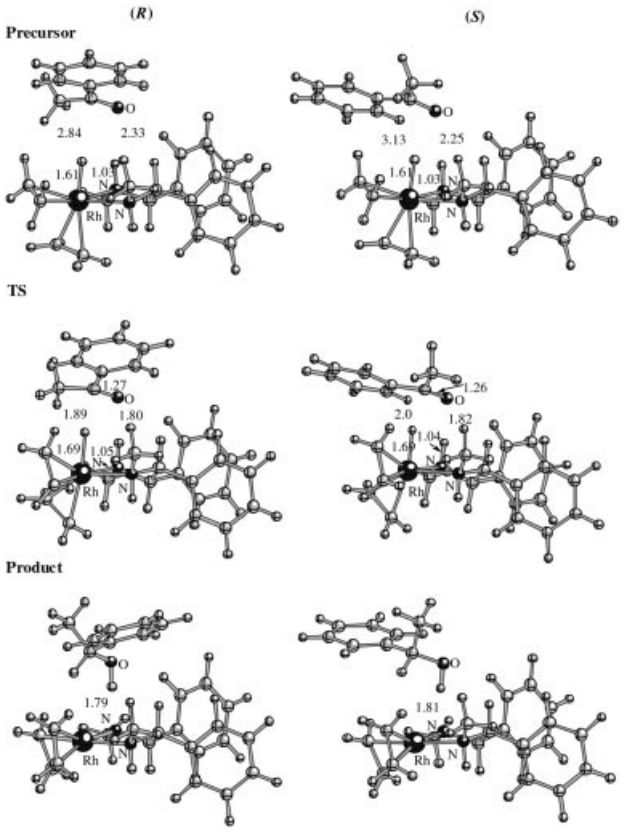

Figure 1. Geometries of the precursor states, of the transition states and of the products for the two diastereoisomeric pathways during the reduction of acetophenone by the Rh^I complex with the experimental (*S*,*S*)-*N*,*N*′-dimethyl-1,2-diphenylethylenediamine ligand

Table 2. Energy (*E*) and energy corrected by the zero-point energy (*E*+ZPE) of the precursor complex, the transition state and the product for the hydrogenation reaction of acetophenone in the case of no substituent on the carbon atoms of the diamine (L = H) and in the case of phenyl substituents (L = Ph); the energies (in kcal/mol) are relative to the sum of the energies of the separated molecules; the pathways leading to the *R* or *S* isomers are compared

		L = H			L = Ph		
		Precursor	TS	Product	Precursor	TS	Product
R isomer							
E	BPW91	−3.9	1.0	−16.1	−3.9	1.0	−15.8
	B3LYP	−6.1	2.1	−18.6			
E+ZPE	BPW91	−3.1	1.6	−13.0	−3.2	1.6	
	B3LYP	−5.2	2.8	−15.1			
S isomer							
E	BPW91	−3.4	2.7	−15.4	−3.5	2.6	−15.2
	B3LYP	−5.7	3.9	−17.4			
E+ZPE	BPW91	−2.6	3.0	−12.4	−3.0	2.4	
	B3LYP	−4.7	4.4	−14.1			

diamine (2.4 Å in both TS). This short distance can indicate the existence of an additional weak hydrogen bond.

3. Energetics of the Reaction

We have calculated the vibrational frequencies for the precursor complexes, the TS and the products, which allows us to correct the energies by the zero-point energy (ZPE). Because of the size of the calculations, only the main species have been considered in the case of L = Ph. The results are given in Table 2. Between the BPW91 and the B3LYP functionals, the energy values differ by 2 kcal/mol but the relative energies between the *R* and the *S* isomers remain the same. With both functionals, the energy of the *R* transition state is smaller than that of the *S* one, in clear relation with the previous geometric discussion: 1.6 vs. 3.0 kcal/mol with BPW91 and 2.8 vs. 4.4 kcal/mol with B3LYP in the case of L = H. When L = Ph, the energies are 1.6 and 2.4 kcal/mol for the *R* and the *S* isomer, respectively, with the BPW91 functional. The energy difference between the two transition states when L = H is 1.4 and 1.6 kcal/mol with BPW91 and B3LYP, respectively. When L = Ph, this difference is 0.8 kcal/mol (with BPW91), then smaller than for L = H. This comes from a stabilization of TS_S compared to TS_R when phenyls are present (3.0 vs. 2.4 kcal/mol), because the presence of phenyls induces a small geometry deformation of the cycle, resulting in a decrease of the steric effects (methyl−methyl interaction) for TS_S.

Hence, at this stage the calculations show that the TS_R transition state leading to the *R* isomer is reached more easily than the TS_S transition state which leads to the *S* isomer: the reaction is enantioselective. However, these results correspond to a reaction in the gas phase, so we then tried to simulate a reaction in solution. Solvent effects have been introduced using the Polarized Continuum Model (PCM) or the Isodensity Surface Polarized Continuum Model (IPCM).[23,24] We took ethanol as solvent to model 2-propanol. With the PCM method, the energy difference between TS_R and TS_S is reduced to 0.23 kcal/mol in the case of L = Ph. When L = H, this difference is also reduced to 0.72 kcal/mol but is increased to 2.8 kcal/mol with B3LYP. With the IPCM method, we obtained oscillatory results. Nevertheless, in both cases, TS_R is more stable than TS_S by 5 kcal/mol with L = H and 1.8 kcal/mol for L = Ph. In conclusion, the enantioselectivity observed in the gas phase is conserved in the calculations simulating the influence of the solvent. However, the energy difference between TS_R and TS_S varies to a large extent. This may be because only single points have been calculated on the geometries obtained for the gas phase. In fact, with such large complexes, it is difficult to reach convergence of the optimizations when the solvent effects are included. Calculations with explicit inclusion of solvent molecules might be required to give more reliable results but they are beyond the scope of this study.

Furthermore the results presented in Table 2 are obtained at 0 K. Therefore we have studied the influence of the temperature on the activation energies, as described below.

4. Kinetic Study

Calculation of the vibrational frequencies allows us to obtain the Gibbs free energy *G* at a given temperature, by an evaluation of the vibrational entropy together with the translational and rotational terms. The first interesting result is that the precursor complexes no longer correspond to a stable state at 298 K and 355 K: the *G* difference between the precursors and the separated fragments is now positive which means that the precursors are only points on the reaction path connecting the separated fragments and the TS. In the precursors, the two interacting fragments are effectively bound together by a hydrogen bond. This corresponds to a loss of entropy and therefore to a destabilization when the entropy is taken into account at room temperature or higher.

A consequence is that the two transition states TS_R and TS_S have the same starting point as reference and their stability difference is the difference of the activation energies $\Delta G^{\#}$. The values for $\Delta G^{\#}$ are given in Table 3. $\Delta G^{\#}_R$ is smaller than $\Delta G^{\#}_S$ in all cases. Their difference is smaller in the case of L = Ph than in the case of L = H (0.6 vs. 1.1 kcal/mol at room temperature). These values can be compared to those obtained previously from zero-point energy corrections *E*+ZPE (0.8 vs. 1.4 kcal/mol). Hence the trend is already correct at this level of calculation and the influence of entropic effects in ΔG is moderate. The comparison between L = Ph and L = H seems to indicate that the substituents on the diamine carbons must not be too bulky, in order not to reduce $\Delta G^{\#}$ too much.

Table 3. Activation free energy $G^{\#}$ (kcal/mol), entropy of the transition states *S* (cal/mol·K), kinetic constant *k* (s^{-1}) and enantiomeric excess *ee* for the hydrogenation reaction of acetophenone in the case of no substituent on the carbons of the diamine (L = H) and in the case of phenyl substituents (L = Ph); the pathways leading to the *R* or *S* isomers are compared

			$G^{\#}_R$	$G^{\#}_S$	S_R	S_S	k_R	k_S	k_R/k_S	ee
L = H	BPW91	298K	15.0	16.1	164.0	164.8	$7.2\,10^1$	$1.1\,10^1$	6.4	73%
		355K	17.6	18.7	181.9	182.7	$1.1\,10^2$	$2.4.10^1$	4.5	63%
	B3LYP	298K	16.6	17.8	161.8	163.6	4.6	0.7	6.6	74%
		355K	19.4	20.4	179.3	181.1	9.3	2.2	4.3	62%
L = Ph	BPW91	298K	15.0	15.6	212.9	214.6	$7.5\,10^1$	$2.7\,10^1$	2.6	44%
		355K	17.6	18.1	238.2	240.1	$1.1\,10^2$	$5.6\,10^1$	1.9	32%

Nevertheless, we can go further and apply the theory of the activated complex which gives the kinetic constant *k* as a function of the free activation energy.[25]

$$k = \frac{k_B T}{h} e^{-\frac{\Delta G^{\ddagger}}{RT}} \quad (1)$$

The values of k_R and k_S calculated at room temperature (298 K) and at 355 K are given in Table 3. The kinetic constants are rather small which means that the reaction is slow. Effectively, it can take several days at 300 K to be complete.[4,7] The enantiomeric excess *ee* can be related to the kinetic constants: in fact it is defined as the ratio of the

difference of the product concentrations to their sum. If it is assumed that the transition states are totally converted into the products, the product concentrations can be replaced by the TS concentrations in the expression for *ee*. The TS concentrations are the product of the reactant concentrations and the kinetic constants. This results in the following expression [Equation (2)]:

$$ee = \frac{[TS_R]-[TS_S]}{[TS_R]+[TS_S]} = \frac{k_R[C_R]-k_S[C_S]}{k_R[C_R]+k_S[C_S]} \quad (2)$$

Since the starting point is the same for the *R* and *S* pathways, the reactant concentration is the same ($[C_R] = [C_S]$) and Equation (2) can be simplified to Equation (3).

$$ee = \frac{k_R - k_S}{k_R + k_S} = \frac{1 - k_S/k_R}{1 + k_S/k_R} \quad (3)$$

$$\frac{k_S}{k_R} = e^{-\frac{\Delta G^{\#}_S - \Delta G^{\#}_R}{RT}} = e^{-\frac{\Delta G_{RS}}{RT}} \quad (4)$$

$$ee = \frac{1 - e^{-\frac{\Delta G_{RS}}{RT}}}{1 + e^{-\frac{\Delta G_{RS}}{RT}}} \quad (5)$$

Thus *ee* can be expressed simply as a function of the free energy difference between the two TS. The *ee* values are given in Table 3 at both temperatures.

Some comments can be made on Table 3.

− In both cases, L = H or Ph and with both functionals, the free activation energy is smaller for TS_R than for TS_S, which can be also formulated by the larger kinetic constant k_R. Therefore the mechanism studied in the present work is enantioselective and yields the *R* isomer. This is also reflected by the values of *ee*. Let us recall that the case L = H is artificially constrained to a single isomer of the diamine ligand otherwise there is no chirality.

− *ee* decreases when the temperature increases. This result has been observed experimentally:[4] when the temperature increases from 25 to 82 °C (298 to 355 K), *ee* decreases by 15%.

− The calculated values for *ee* are close to the experimental ones: 50% in the conditions of Scheme 1 with ethylene as ligands.[9] Of course we must consider this agreement with care, owing to the limited accuracy of the computational approach: for instance limitations of DFT functionals, calculation of *ee* for the gas phase. Nevertheless our results show that DFT calculations can correctly reproduce the experimental results.

We will now comment on the role of entropy. The values of the transition-state entropy are also given in Table 3. The entropy of TS_S is always larger than that of TS_R. This reflects the fact that TS_S is earlier, with the two reactants less bound together. Hence the entropy gain when the temperature increases is smaller for the *R* isomer, which explains why the difference of the activation free energies, the ratio of the kinetic constants and the enantiomeric excesses diminish when the temperature increases.

IV. Conclusion

The theoretical work presented here represents a complete study of the mechanism of asymmetric ketone hydrogenation by a Rh^I complex. It has allowed us to determine the factors influencing the enantioselectivity. The important conclusions are:

− Only one mechanism can account for the enantioselectivity of the reaction. This is a concerted mechanism where two hydrogens are simultaneously transferred to the ketone: the hydride and one hydrogen carried by one of the diamine nitrogen atoms. Thus the amines must not be tertiary amines.

− To ensure enantioselectivity, only one hydrogen must point toward the Rh−H bond, which means that the diamine must have a C_2 symmetry axis. This eliminates the primary amines also.

− Furthermore this configuration must be unique since a mixture of diastereoisomers of the starting complex would lead to a racemic reaction. This is ensured by the presence of bulky substituents, such as phenyl groups, on the diamine asymmetric carbon atoms.

− Nevertheless, the substituents must not be too bulky, since we have seen that the enantiomeric excess is better with smaller substituents on the carbons. A compromise must hence be found with the previous argument.

In conclusion, we have shown in this work that DFT calculations are a very useful tool for explaining mechanisms. Our results show that important insights can be obtained with such a theoretical approach, particularly the origin of the reaction asymmetry. This can help experimentalists to choose substituents that will ensure good enantioselectivity.

Acknowledgments

The authors thank the Institut du Développement et des Ressources en Informatique Scientifique (IDRIS) at Orsay, the Centre Informatique National de l'Enseignement Supérieur (CINES) at Montpellier and the Pôle de Modélisation et de Simulation Numérique (PSMN) at ENS Lyon for CPU time.

[1] G. Zassinovich, G. Mestroni, S. Gladiani, *Chem. Rev. (Washington, DC)* **1992**, *92*, 1051.
[2] S. Gladiani, G. Mestroni, in: *Transition Metals for Organic Synthesis, Vol. 2* (Eds.: M. Beller, C. Bolm), Wiley-VCH, Weinheim, Germany, **1998**, p. 97.
[3] P. Gamez, F. Fache, P. Mangeney, M. Lemaire, *Tetrahedron Lett.* **1993**, *34*, 6897.
[4] P. Gamez, F. Fache, M. Lemaire, *Tetrahedron: Asymmetry* **1995**, *6*, 705.
[5] P. Gamez, B. Dunjic, F. Fache, M. Lemaire, *Tetrahedron: Asymmetry* **1995**, *6*, 1109.
[6] F. Fache, P. Gamez, F. Nour, M. Lemaire, *J. Mol. Cat.* **1993**, *85*, 131.
[7] F. Touchard, M. Bernard, F. Fache, F. Delbecq, V. Guiral, P. Sautet, M. Lemaire, *J. Organomet. Chem.* **1998**, *567*, 133.

[8] [8a] S. Hashigushi, A. Fujii, J. Takehara, T. Ikariya, R. Noyori, *J. Am. Chem. Soc.* **1995**, *117*, 7562. [8b] R. Noyori, S. Hashiguchi, *Acc. Chem. Res.* **1997**, *30*, 97.
[9] M. Bernard, V. Guiral, F. Delbecq, F. Fache, P. Sautet, M. Lemaire, *J. Am. Chem. Soc.* **1998**, *120*, 1441.
[10] K.-J. Haack, S. Hashiguchi, A. Fujii, T. Ikariya, R. Noyori, *Angew. Chem. Int. Ed. Engl.* **1997**, *36*, 6.
[11] K. Abdur-Rashid, M. Faatz, A. J. Lough, R. H. Morris, *J. Am. Chem. Soc.* **2001**, *123*, 7473.
[12] C. de Bellefon, N. Tanchoux, *Tetrahedron: Asymmetry* **1998**, *9*, 3677.
[13] M. Yamakawa, H. Ito, R. Noyori, *J. Am. Chem. Soc.* **2000**, *122*, 1466.
[14] D. A. Alonso, P. Brandt, S. J. M. Nordin, P. G. Andersson, *J. Am. Chem. Soc.* **1999**, *121*, 9580.
[15] V. Guiral, F. Delbecq, P. Sautet, *Organometallics* **2000**, *19*, 1589.
[16] V. Guiral, F. Delbecq, P. Sautet, *Organometallics* **2001**, *20*, 2207.
[17] *Gaussian 98* (Revision A.7), M. J. Frisch, G. W. Trucks, H. B. Schlegel, G. E. Scuseria, M. A. Robb, J. R. Cheeseman, V. G. Zakrzewski, J. A. Montgomery, R. E. Stratmann, J. C. Burant, S. Dapprich, J. M. Millam, A. D. Daniels, K. N. Kudin, M. C. Strain, O. Farkas, J. Tomasi, V. Barone, M. Cossi, R. Cammi, B. Mennucci, C. Pomelli, C. Adamo, S. Clifford, J. Ochterski, G. A. Petersson, P. Y. Ayala, Q. Cui, K. Morokuma, D. Malick, A. D. Rabuck, K. Raghavachari, J. B. Foresman, J. Cioslowski, J. V. Ortiz, B. B. Stefanov, G. Liu, A. Liashenko, P. Piskorz, I. Komaromi, R. Gomperts, R. L. Martin, D. J. Fox, T. Keith, M. A. Al-Laham, C. Y. Peng, A. Nanayakkara, C. Gonzalez, M. Challlacombe, P. M. W. Gill, B. G. Johnson, W. Chen, M. W. Wong, J. L. Andres, M. Head-Gordon, E. S. Replogle, J. A. Pople, Gaussian, Inc., Pittsburgh PA, **1998**.
[18] P. J. Hay, W. R. Wadt, *J. Chem. Phys.* **1985**, *85*, 299.
[19] Y. Bouteiller, C. Mijoule, M. Nizam, J. C. Barthelat, J. P. Daudey, M. Pelissier, *Mol. Phys.* **1988**, *65*, 295.
[20] Y. Bouteiller, C. Mijoule, M. Nizam, J. C. Barthelat, J. P. Daudey, M. Pelissier, private communication.
[21] C. Peng, H. B. Schlegel, *Israel J. Chem.* **1993**, *33*, 449.
[22] M. Bernard, V. Guiral, F. Delbecq, F. Fache, P. Sautet, M. Lemaire, *Organometallics* **2000**, *19*, 5715.
[23] V. Barone, M. Cossi, J. Tomasi, *J. Comp. Chem.* **1998**, *19*, 404 and refs. therein.
[24] J. B. Foresman, T. A. Keith, K. B. Wiberg, J. Snoonian, M. J. Frisch, *J. Phys. Chem.* **1996**, *100*, 16098.
[25] S. W. Benson, *Thermochemical Kinetics*, 2nd ed., John Wiley & Sons, New York, **1976**, p. 94.

Received December 16, 2002

